This is the accepted manuscript made available via CHORUS. The article has been published as:

Predicted multiple Walker breakdowns for current-driven domain wall motion in antiferromagnets

Mu-Kun Lee, Rubén M. Otxoa, and Masahito Mochizuki

Phys. Rev. B **110**, L020408 — Published 31 July 2024

DOI: 10.1103/PhysRevB.110.L020408

Predicted Multiple Walker Breakdowns for Current-Driven Domain-Wall Motion in Antiferromagnets

Mu-Kun Lee,[1] Rubén M. Otxoa,[2,3] and Masahito Mochizuki[1]

[1]*Department of Applied Physics, Waseda University, Okubo, Shinjuku-ku, Tokyo 169-8555, Japan*
[2]*Hitachi Cambridge Laboratory, J. J. Thomson Avenue, Cambridge CB3 OHE, UK*
[3]*Donostia International Physics Center, paseo Manuel de Lardizabal 4, 20018 San Sebastián, Spain*

We theoretically discover possible emergence of reentrant Walker breakdowns for current-driven domain walls in layered antiferromagnets in striking contrast to the unique Walker breakdown in ferromagnets. We reveal that the Lorentz contraction of domain-wall width in antiferromagnets gives rise to nonlinear current-dependence of the wall velocity and the predicted multiple Walker breakdowns. The dominant efficiency of the current-induced staggered spin-orbit torque over the spin-transfer torque to drive the domain-wall motion is also demonstrated. These findings are expected to be observed in synthetic antiferromagnets experimentally and provide an important contribution to the growing research field of antiferromagnetic spintronics.

PACS numbers:

Introduction.—Spintronics based on antiferromagnets has attracted significant attention in recent decades. Compared with ferromagnets, antiferromagnets possess several advantages for spintronics application, including the absence of stray fields and high-speed operation in terahertz domains [1, 2]. Methods for manipulating and detecting spin textures in antiferromagnets including domain walls (DWs), skyrmions, bimerons, etc., have been proposed [3–12]. It is known that a moving ferromagnetic DW suffers from Walker breakdown when driven by large current or strong magnetic field, beyond which the DW oscillates between the Bloch and Néel types and its velocity is suppressed [13, 14]. Recently, it has been proposed that the antiferromagnetic DW is immune to Walker breakdown and the maximal DW speed is limited by the magnon velocity, which is, however, much higher than the breakdown threshold velocity in ferromagnets [15–19].

In this work, we theoretically study the current-driven motion of DWs in layered antiferromagnets with antiferromagnetically stacked ferromagnetic layers. We cosnider effects of both the spin-transfer torque (STT) and the staggered field-like spin-orbit torque (SOT) exerted by electric currents. We first demonstrate overwhelming efficiency of SOT over STT to drive the DW motion by numerical simulations. Then we construct an analytical theory to explain this nontrivial result and reveal the Lorentz contraction of DW as its physical origin. We further find that this DW contraction gives rise to reentrant emergence of Walker breakdowns separated by multiple Walker regimes in which the rigid DW motion is supported. It is found that the upper limit of DW speed is still governed by magnon velocity when the Lorentz invariance manifests. Averaged DW velocities in the breakdown regimes are calculated as another prediction for future experiments. Our findings are expected to be observed in synthetic antiferromagnets [5, 6].

Domain wall velocity.—We consider antiferromagnetically stacked one-dimensional Néel DWs shown in Fig. 1(a). The Hamiltonian for this system is given by,

$$\mathcal{H} = \sum_i \Big[- J_{\rm F} \boldsymbol{m}_i \cdot \boldsymbol{m}_{i+\hat{x}} + J_{\rm AF} \boldsymbol{m}_i \cdot \boldsymbol{m}_{i+\hat{y}} + K_{\rm h} m_{iy}^2 - K_{\rm e} m_{iz}^2 \Big], \tag{1}$$

where $\boldsymbol{m}_i (= \boldsymbol{M}_i/M)$ is the normalized magnetization vector at the ith site, $\boldsymbol{M}_i$ is the magnetization, and M is its norm. Here $J_{\rm F}$ ($J_{\rm AF}$) is the (anti)ferromagnetic exchange coupling, and $K_{\rm e}$ ($K_{\rm h}$) is the easy (hard) magnetization anisotropy along the z (y) axis. This Hamiltonian is a simplified model of Mn_2Au [4, 20, 21] and CuMnAs [3].

We simulate the current-induced DW motion by using the Landau-Lifshitz-Gilbert-Slonczewski (LLGS) equation [22–25], $\partial_t \boldsymbol{M}_i = -\gamma \boldsymbol{M}_i \times [\boldsymbol{B}_i^{\rm eff} + (-1)^{i_y} B_{\rm SO} \hat{\boldsymbol{z}}] + \frac{\alpha}{M} \boldsymbol{M}_i \times \partial_t \boldsymbol{M}_i - (\boldsymbol{u} \cdot \boldsymbol{\nabla}) \boldsymbol{M}_i + \frac{\beta}{M} \boldsymbol{M}_i \times (\boldsymbol{u} \cdot \boldsymbol{\nabla}) \boldsymbol{M}_i$. Here $\alpha (= 0.001)$ is the Gilbert-damping coefficient, and β is the strength of nonadiabatic torque. We introduce the current vairable $\boldsymbol{u} \equiv p\gamma\hbar a_0^3 \boldsymbol{j}_{\rm e}/(2eM)$ where $\boldsymbol{j}_{\rm e} = j_{\rm e}\hat{\boldsymbol{x}}$ is the electric current density vector, $p (= 0.5)$ is the spin polarization of the current, a_0 is the lattice constant, $\gamma (= g\mu_{\rm B}/\hbar)$ is the gyromagnetic ratio. The effective local magnetic field is calculated by $\boldsymbol{B}_i^{\rm eff} = -\partial \mathcal{H}/\partial \boldsymbol{M}_i$. The current-induced SO-field $\boldsymbol{B}_{\rm SO}$ alternates between the layers stacked in the y direction [4, 20]. The parameter values are set to be those of Mn_2Au (see Sections (Sec.) I and II in [26]).

The injected electric current exerts both SOT and STT simultaneously to magnetizations constituting DW in each layer. Strength of the field-like SOT $B_{\rm SO}$ is proportional to the current density as $B_{\rm SO} = f_{\rm SO} j_{\rm e}$. The density-functional calculations evaluated the coefficient as $f_{\rm SO} \approx 2 \times 10^{-10}$ T cm^2/A for Mn_2Au [3]. Here, we assume a constant $f_{\rm SO}$ for all the current-density ranges. A previous study examined the DW motion driven by SOT only [20]. On the contrary, we investigate the current-

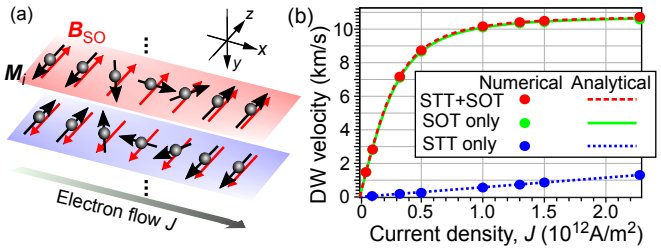


FIG. 1: (a) Schematics of the system. (b) Numerical and analytical results of the DW velocities.

density dependence of DW velocity in the presence of (i) only STT, (ii) only SOT, and (iii) both STT and SOT to compare the effects of SOT and STT on equal footing [Fig. 1(b)]. In the simulations, we take a rather unphysically large value of β as $\beta = 10\alpha$ on purpose, with which the effect of STT should be prominent. Even in this extreme condition, the contribution of STT to DW motion is still much smaller than that of SOT. For instance, when $j_e = 1.3 \times 10^{12}$ A/m^2, the velocity driven solely by STT ($v_{\rm STT} \approx 0.75$ km/s) is only approximately 7% of that by SOT ($v_{\rm SOT} \approx 10.4$ km/s). This result demonstrates an overwhelming efficiency of SOT for driving the DW motion. Intriguingly, when both torques coexist, the DW velocity ($v_{\rm both} \approx 10.5$ km/s) is not given by a simple addition of these two velocities ($v_{\rm STT}+v_{\rm SOT} \approx 11.12$ km/s), although both torques should work additively [13]. To explain this phenomenon, we analytically derive the formula of DW velocity [plotted with lines in Fig. 1(b)] by employing a simple two-layer model with presumed rigid DW profiles during the motion [5, 13]. The DW profiles are obtained from the saddle-point equation of the Hamiltonian as $\boldsymbol{M}_l = M(\sin\theta_l\cos\phi_l, \sin\theta_l\sin\phi_l, \cos\theta_l)$ with $\theta_{\rm L} = -2\tan^{-1}[\exp\frac{x-q(t)}{\Delta}]$ and $\theta_{\rm U} = \theta_{\rm L} + \pi$, where l(=U, L) is an index of the upper and lower layers. Here $q(t)$ and Δ are the center coordinate and the width of the DW, respectively, and the tilt angle $\phi_l(t)$ is assumed to be spatially uniform [5, 13]. We plugged this formula into LLGS equation and confirmed that the DWs in the upper and lower layers have common $q(t)$ and Δ when the antiferromagnetic coupling $J_{\rm AF}$ is sufficiently strong.

After some algebra, we obtain $\phi_{\rm L} = -\phi_{\rm U}$ and $\dot{\phi}_{\rm U}(1+\alpha^2) = u(\alpha-\beta)/\Delta - \gamma B_{\rm SO} - \alpha\gamma(J_{\rm AF}+K_{\rm h})\sin(2\phi_{\rm U})/M$, showing a competition between STT, SOT, and antiferromagnetic exchange plus anisotropy torques. The condition for terminally static ϕ_l, namely $\dot{\phi}_{\rm U} = 0$, is

$$\sin(2\phi_{\rm U}) \;=\; -\frac{M}{\alpha\gamma(J_{\rm AF}+K_{\rm h})}\Big[\frac{u(\beta-\alpha)}{\Delta} + \gamma B_{\rm SO}\Big]. \quad (2)$$

Note that this formula has the same form as that in a ferromagnetic thin film lying on the xy plane [13], where $J_{\rm AF} + K_{\rm h}$ plays the same role as the demagnetization factor $N_y - N_x$ in the latter case. Therefore, we expect Walker breakdown to occur also in the layered antiferromagnets [13, 20]. Using Eq. (2), the DW velocity is derived as

$$v \equiv \dot{q} \;=\; u\frac{\beta}{\alpha} + \frac{\gamma B_{\rm SO}\Delta}{\alpha}. \quad (3)$$

The right-hand side is a sum of two contributions from STT (the first term as in [27]) and SOT (the second term). We, therefore, naively expect that the DW velocity v in the presence of both STT and SOT is given by a simple sum as $v_{\rm both} = v_{\rm STT} + v_{\rm SOT}$ where $v_{\rm STT}$ ($v_{\rm SOT}$) is the velocity in the presence of STT (SOT) only. We also expect that v is proportional to u or the current density j_e because $B_{\rm SO} \propto u$. However, the normalized staggered magnetization $\boldsymbol{l} \equiv (\boldsymbol{M}_{\rm U} - \boldsymbol{M}_{\rm L})/2M$ in antiferromagnets follows the Lorentz-invariant equation of motion when the damping and the current-induced torques are compensated, and thus the DW width Δ suffers from a relativistic contraction [15, 17, 28] as $\Delta(v) \approx \Delta_0\sqrt{1-v^2/v_g^2}$, where $\Delta_0(=a_0\sqrt{J_{\rm F}/2K_{\rm e}})$ is the DW width in the static case and $v_g(=a_0\sqrt{J_{\rm F}J_{\rm AF}}/\hbar)$ is the magnon velocity in the exchange limit ($|\boldsymbol{m}| \equiv |(\boldsymbol{M}_{\rm U}+\boldsymbol{M}_{\rm L})/2M| \ll |\boldsymbol{l}|$, see Sec. IX in [26]). Therefore, $v_{\rm both}$ should depend nonlinearly on the current density u and the SO-field $B_{\rm SO}$, and the velocity is no longer given by a simple addition of $v_{\rm STT} + v_{\rm SOT}$.

With the formula of the Lorentz-contracted width $\Delta(v)$, Eq. (3) becomes a quadratic equation for v. One solution of this equation is negative and, thus, is unphysical because $\boldsymbol{j}_e \propto +\hat{\boldsymbol{x}}$ gives rise to a net torque that should drive DW motion in the $+\hat{\boldsymbol{x}}$ direction (see Sec. VII in [26]). The other solution is positive and thus is physical, which can be simplified as $v = u/(a\sqrt{c+du^2} - b)$ with constants $a = \gamma f_{\rm SO}/(FJ_{\rm AF})$, $b = 2K_{\rm e}\alpha\beta/F$, $c = 2J_{\rm AF}^2 J_{\rm F}K_{\rm e}(a_0\alpha)^2$, $d = J_{\rm AF}\hbar^2F$, and $F = J_{\rm F}(\gamma f_{\rm SO}a_0)^2 - 2K_{\rm e}\beta^2$. This simple analytical solution is the first major result of this study, which is shown by lines in Fig. 1(b) and coincides well with the numerical results. We show an alternative derivation based on the Thiele equation [29] in Sec. X in [26], which turns out to give the same formula for the DW velocity.

When $B_{\rm SO} = 0$, v is independent of $J_{\rm AF}$, which can be understood intuitively. A finite $B_{\rm SO}$ efficiently tilts $\boldsymbol{M}_l$ on both layers along the hard axis $-\hat{\boldsymbol{y}}$ direction (see Sec. VII in [26]). Subsequently, the $J_{\rm AF}$ coupling induces a strong exchange torque owing to this tilt to drive DW motion [21]. This scenario is the same as that in the synthetic antiferromagnets [5], where the damping-like SOT is the dominant mechanism for the high DW speed. Note that Eq. (2) indicates that there is still a finite tilt angle even when $B_{\rm SO} = 0$ owing to the STT. The DW velocity in this case is proportional to $(J_{\rm AF}+K_{\rm h})\Delta\sin(2\phi_{\rm U})$ (see Sec. II in [26]), and thus, the dependence on $J_{\rm AF}$ is cancelled, resulting in effectively uncoupled ferromagnetic DWs. In addition, in the limit of $u \to \infty$, we obtain $v \to v_g\sqrt{1-n}$, with $n = \frac{2K_{\rm e}}{J_{\rm F}}(\frac{\beta}{\gamma f_{\rm SO}a_0})^2 \approx 4\times10^{-4}$ using

$\beta = 10\alpha$. Therefore, we find that the DW velocity cannot exceed the magnon velocity v_g as expected and can reach v_g only in the adiabatic limit of $\beta = 0$.

Magnon velocity and tilt angle.—We use a saddle-point solution of $\theta_{\mathrm{U,L}}$ to fit the simulated DW widths and evaluate v_g numerically, which is close to the analytical value (see Sec. III in [26]). For $j_e = 1.5 \times 10^{12}$ A/m^2, Eq. (2) leads to $\sin(2\phi_{\mathrm{U}}) \approx -0.16$, and the DWs are within Walker regime to maintain the rigid moving profiles, which self-consistently justifies our initial substitution of the rigid DW profiles into the LLGS equation. This corresponds to $M_{\mathrm{U/L},y} \approx -0.08 M \mathrm{sech}(\frac{x-vt}{\Delta(v)})$ with the same sign for both layers. This analytical result coincides well with the simulation results (see Sec. III in [26]). The minor discrepancy in the peak height is attributable to nonzero spin-wave emissions behind the moving DW indeed observed in the simulations.

Prediction of multiple Walker regimes.— The Walker breakdown is defined as a regime in which rigid DW profiles are no longer stable when driven by large current or strong field exceeding a threshold, with which $\dot{\phi}_{\mathrm{U,L}}$ becomes finite. In the breakdown regime, the right-hand side of Eq. (2) is greater than 1 or less than -1, and thus the threshold current u_c is determined by the condition $\sin(2\phi_{\mathrm{U}}(u_c)) = \pm 1$. It has been widely believed that the Walker breakdown should not occur for DWs in antiferromagnets [15–19]. However, we find that it can occur in layered antiferromagnets with exchange coupling J_{AF} because Eqs. (2) and (3) have the same form as that for DWs in ferromagnetic thin films [13]. Substituting the analytical solution of v into Eq. (2), we obtain its u-dependence as $\sin(2\phi_{\mathrm{U}}) = -c_0 u\left[1 + \frac{(\beta-\alpha)(c_1+c_2u^2)}{x_1\sqrt{1+c_5u^2}-x_2u^2}\right]$ with coefficients specified in Sec. IV in [26]. This indicates nonlinear u dependence of $\sin(2\phi_{\mathrm{U}})$ and possible emergence of multiple Walker regimes separated by breakdown regimes with boundaries defined by $\sin(2\phi_{\mathrm{U}}(u_c)) = \pm 1$. This is in striking contrast to the case of ferromagnets, in which $\sin(2\phi)$ shows a monotonic behavior against u and, thus, only a unique threshold current density appears [13, 14].

For better data visualization, Fig. 2 shows the current-density dependence of $\sin(2\phi_{\mathrm{U}})$ when $\alpha = 0.005, \beta = 0.5\alpha$, and $J_{\mathrm{AF}} = 10^{-3} J_{\mathrm{AF,Mn_2Au}}$ with $J_{\mathrm{AF,Mn_2Au}}$ being the AF exchange coupling in Mn_2Au, in which we find multiple Walker regimes in (i) $0 < u < u_{c1}$ with $u_{c1} \approx u_0$ and (ii) $u_{c2} < u < u_{c3}$ with $u_{c2} \approx 5.4u_0$ and $u_{c3} \approx 6.3u_0$, where $u_0 \equiv (p\gamma\hbar a_0^3/2eM) \times 10^{12}$ A/m^2. There is a singular point of $\sin(2\phi_{\mathrm{U}})$ at $u_s = v_g\alpha/\beta \approx 11.8u_0$, at which the denominator vanishes as $x_1\sqrt{1+c_5u^2} - x_2u^2 = 0$ that causes $\sin(2\phi_{\mathrm{U}})$ abruptly crosses from a positive to a negative value. This u_s is a criterion of u for the stability of DW. Equation (3) leads to $\Delta = (\alpha v - \beta u)/\gamma f_{\mathrm{SO}} u$. At the singular current, $\Delta(u_s) = (\alpha v(u_s) - \beta u_s)/\gamma f_{\mathrm{SO}} u_s \leq (\alpha v_g - \beta u_s)/\gamma f_{\mathrm{SO}} u_s = 0$, thus the DW already shrinks to zero width before the current reaches u_s. Therefore, for current $u > u_s$, even if there is a self-consistent Walker regime, it does not support a stable DW. The equation for the threshold current, $\sin(2\phi_{\mathrm{U}}(u_c)) = \pm 1$, has no analytical solutions since it has a form $\sum_{n=1}^{6} \gamma_n u_c^n = 0$ with the sixth-order polynomial of u_c and coefficients γ_n. Nevertheless, it evidently implies that more than one Walker regimes can exist. This is another central result of this work. Note that there is also self-consistent solution of multiple Walker breakdowns when $\beta > \alpha$ (see Sec. IV in [26]), but it cannot be observed since the second Walker regime occurs at currents larger than u_s. For $\alpha = \beta$, only a single breakdown regime appears similar to the ferromagnetic case, which leads to $\sin(2\phi_{\mathrm{U}}) = -c_0 u$ and a unique threshold current density of $u_c = 1/c_0$.

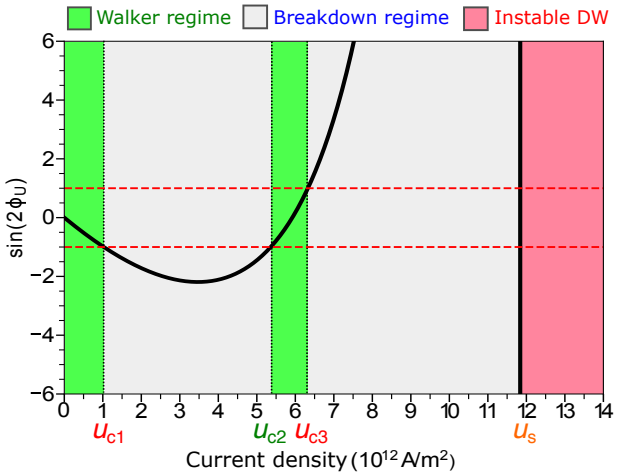


FIG. 2: Thick solid (black) curves show $\sin(2\phi_{\mathrm{U}})$ when $\beta = 0.5\alpha$. Horizontal dotted lines label the values ± 1. Grey areas indicate the Walker breakdown regimes, and red area the instable DW regime.

The physical mechanism of reentrant Walker regime can be seen by the equation of $\dot{\phi}_{\mathrm{U}}$ in the paragraph above Eq. (2). The strength of STT due to angular momentum conservation when electrons pass through the DW is proportional to u/Δ which characterizes the rate of electron spin reverse, since Δ is the length scale of local magnetization reverse in a DW, and u relates to polarized electron's velocity. Due to the Lorentz contraction of Δ in antiferromagnets, the competition between STT ($\propto u/\Delta$) and SOT ($\propto u$) can bend the right-hand side of Eq. (2) from less than -1 to exactly -1, driving the DW from breakdown into second Walker regime, as confirmed by numerical integration of LLGS equation with fourth-order Runge-Kutta (RK) method (see Sec. V in [26]).

Averaged velocity in breakdown regime.—In breakdown regime, $\phi_{\mathrm{U,L}}(t)$ depends on time such that both $\sin(2\phi_{\mathrm{U,L}}(t))$ and $v(t)$ oscillate in time, and it is no longer permissible to use Eq. (2) to obtain Eq. (3). From RK calculation (see Sec. VI in [26]), we get the time-averaged DW velocity as shown in black dots in Fig. 3. Besides a quantitative agreement with the analytical velocities in

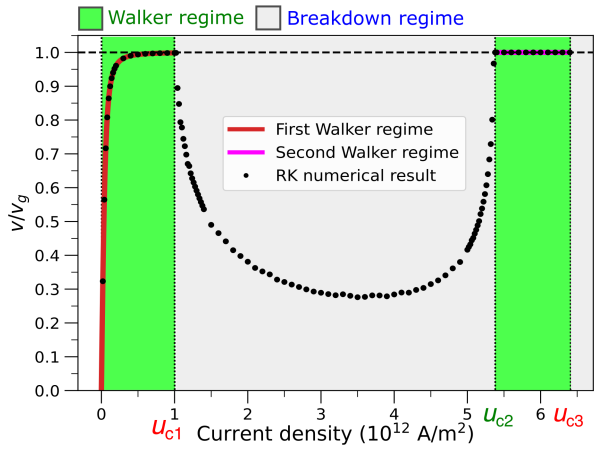


FIG. 3: Curves represent analytical DW velocities in Walker regimes, and dots represent terminal (time-averaged) velocities in Walker (breakdown) regimes by RK calculation.

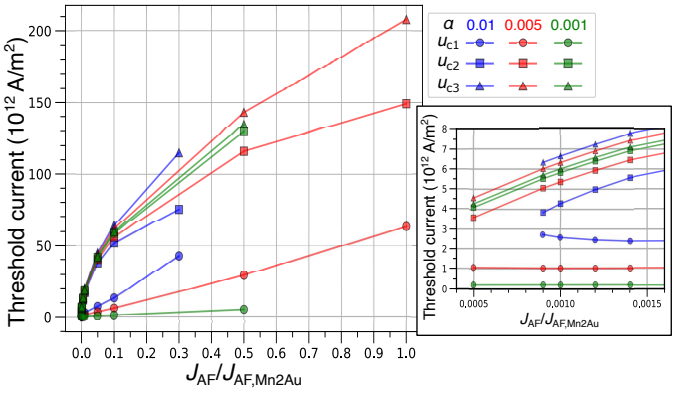


FIG. 4: Threshold currents as functions of the interlayer antiferromagnetic coupling for various Gilbert dampings. Inset shows enlarged view.

Walker regimes, in breakdown regime we find a drop of time-averaged velocity similar to the case in ferromagnets [13, 14].

There is an intuitive way to expect this velocity drop in breakdown regime. In the presence of STT and staggered SOT, we can extend the consideration in [30–32] to write the Lagrangian density for our layered antiferromagnet as,

$$\mathcal{L} = -\mathcal{J}\boldsymbol{m}\cdot[\boldsymbol{l}\times(\partial_t + u\partial_x)\boldsymbol{l}] - 4J_{\rm AF}\boldsymbol{m}^2/a_0 - \mathcal{U}(\boldsymbol{l}), \quad (4)$$

where $\mathcal{J} = M/\gamma a_0$ and $\mathcal{U} = J_{\rm F}a_0(\partial_x\boldsymbol{l})^2 - K_{\rm e}l_z^2/a_0 + K_{\rm h}l_y^2/a_0 - (M/a_0)\boldsymbol{l}\cdot\boldsymbol{B}_{\rm SO}$ is the energy density of $\boldsymbol{l}$. The $\mathcal{J}$ term is the spin Berry phase in a gauge with opposite Dirac strings $\boldsymbol{n}_{0,l}$ for the two sublattices in the monopole representation $\sum_l \mathcal{L}_{{\rm B},l} = \frac{1}{\gamma a_0}\sum_l[\boldsymbol{n}_{0,l}\cdot\boldsymbol{M}_l\times(\partial_t + u\partial_x)\boldsymbol{M}_l]/(1-\boldsymbol{n}_{0,l}\cdot\boldsymbol{M}_l)$ and is expanded up to the second order of $\boldsymbol{m}$. (The next finite order of $\boldsymbol{m}$ is the third order which can be proved by choosing, e.g., $\boldsymbol{n}_0 = \pm\hat{\boldsymbol{z}}$ for the two sublattices, respectively.) [30, 31]. The adiabatic STT contributes to the second term of the convective derivative $(\partial_t + u\partial_x)$ [33]. Neglecting the nonadiabatic STT and Rayleigh dissipation ($\propto \alpha\dot{\boldsymbol{m}}^2$), we obtain $\boldsymbol{m} = -\mathcal{J}a_0\boldsymbol{l}\times(\partial_t + u\partial_x)\boldsymbol{l}/(8J_{\rm AF})$ from the Lagrange equation. Using the saddle-point DW profile of $\boldsymbol{l}$, the $\boldsymbol{m}$-dependent terms after integrating over x become $\frac{M_0}{2}(v-u)^2 + \frac{I}{2}\dot{\phi}_{\rm U}^2$, which are the translational and rotational kinetic energies of a soliton with mass $M_0 = M^2/(4\gamma^2 a_0\Delta J_{\rm AF})$ and moment of inertia $I = M_0\Delta^2$. In this derivation, we assume a time-independent terminal Δ.

Near $u_{\rm c1} \approx 0.06$ km/s, v is close to $v_g \approx 0.34$ km/s, thus $v(u_{\rm c1})$ is greater than $u_{\rm c1}$. When the system crosses the threshold $u_{\rm c1}$ and enters the breakdown regime, the soliton angular frequency $\dot{\phi}_{\rm U}$ changes abruptly from zero to finite, which causes a nonzero rotational energy. To preserve the kinetic energy of the soliton in a narrow current-density range near $u_{\rm c1}$, the DW velocity should decrease as Fig. 3 shows. From the experimental point of view, however, it should be mentioned that with currents close to $u_{\rm c1}$, several other instabilities and effects may appear such as spin-wave emissions [34] and DW proliferations [20] (SI. Sec. VII). Indeed, it was theoretically argued that an effective gyrofield induced by the kinetic energies of DW can cause the DW proliferation together with the transient Lorentz-invariance breaking with DW speeds exceeding v_g [20, 35].

Proposal for experimental observations.—In synthetic antiferromagnets [5, 6], an underlying Pt layer induces a damping-like SOT $\propto \boldsymbol{M}\times\boldsymbol{M}\times\hat{\boldsymbol{z}}$ (using our coordinate convention) in the same direction but with different strengths for the two magnetic layers on top of it (stacked along $-\hat{\boldsymbol{y}}$) [5]. One can fabricate another Pt layer above the upper magnetic layer which, by symmetry, generates an opposite SOT when applying the current. In this situation, each layer is driven by opposite damping-like SOT. After taking a curl product of the LLGS equation with $\boldsymbol{M}$ to cancel time derivatives on its right-hand side, it induces a staggered field-like SOT $\propto \pm\boldsymbol{M}\times(\boldsymbol{M}\times\boldsymbol{M}\times\hat{\boldsymbol{z}}) \propto \mp\boldsymbol{M}\times\hat{\boldsymbol{z}}$, which mimics the staggered SO-field $\boldsymbol{B}_{\rm SO}$ in our case. Therefore, we expect similar results of multiple Walker breakdowns to occur in synthetic antiferromagnets with both top and bottom Pt layers.

Since $J_{\rm AF}$ can be tuned in synthetic antiferromagnets by changing the thickness of metallic layer sandwiched by two magnetic layers, we investigate the dependence of $u_{{\rm c}j}$ on $J_{\rm AF}$ as well as the Gilbert damping α when $\beta = 0.5\alpha$ with other parameters following that of Mn_2Au. The results plotted in Fig. 4 show nearly monotonic decrease of $u_{{\rm c}j}$ as $J_{\rm AF}$ decreases, since a smaller antiferromagnetic exchange torque requires a smaller STT (and thus smaller $u_{{\rm c}j}$) to compensate as shown in the equation for $\dot{\phi}_{\rm U}$ above Eq. (2). It requires roughly $J_{\rm AF} \le 10^{-3}J_{{\rm AF},{\rm Mn_2Au}}$ to get experimentally feasible current below $\sim 10^{13}$ A/m^2

to observe the second Walker regime. We have checked the Lorentz contraction of DW width still manifests in this small exchange regime by micromagnetic simulation. Moreover, for larger dampings, second Walker regime between u_{c2} and u_{c3} appears in a wider range, appropriate for experimental observations, although one should note that for $\alpha = 0.01$, there is no longer real solution of u_{cj} for $J_{\rm AF} < 9 \times 10^{-4} J_{\rm AF,Mn_2Au}$ in our parameter set.

Conclusion.—We have theoretically studied the DW motion in layered antiferromagnets driven by electric current, which exerts both STT and staggered SOT. We have discovered possible reentrant emergence of multiple Walker breakdowns, which is in sharp contrast to the unique Walker breakdown for the current-driven DW motion in ferromagnets. We have revealed that the Lorentz contraction of DW width in antiferromagnets gives rise to nonlinear current-dependence of the DW velocity and the predicted multiple Walker breakdowns. The dominant efficiency of SOT over STT and their non-additive effects in driving the DW motion have been also demonstrated. It should be mentioned that the present theory can be generalized in the straightforward way for intrinsic antiferromagnetic systems in which STT is not applicable or for the cases in which other torques due to additional effects are present (e.g., Dzyaloshinskii-Moriya interaction, Rashba spin-orbit interaction, spin Hall effect). Our findings are expected to be observed in synthetic antiferromagnets experimentally and provide siginificant contributions to development of the antiferromagnetic spintronics.

This work is supported by Japan Society for the Promotion of Science KAKENHI (Grant No. 20H00337 and No. 23H04522), CREST, the Japan Science and Technology Agency (Grant No. JPMJCR20T1) , and the Waseda University Grant for Special Research Project (Project No. 2023C-140). M.K.L. is grateful for illuminating discussions with Rintaro Eto, Collins A. Akosa, and Xichao Zhang.

[1] T. Jungwirth, X. Marti, P. Wadley, and J. Wunderlich, Antiferromagnetic spintronics, Nat. Nanotech. **11**, 231 (2016).
[2] E. V. Gomonay and V. M. Loktev, Spintronics of antiferromagnetic systems, Low Temp. Phys. **40**, 17 (2014).
[3] P. Wadley, B. Howells, J. Zlezný, C. Andrews, V. Hills, R. P. Campion, V. Novák, K. Olejník, F. Maccherozzi, S. S. Dhesi, S. Y. Martin, T. Wagner, J. Wunderlich, F. Freimuth, Y. Mokrousov, J. Kuneš, J. S. Chauhan, M. J. Grzybowski, A. W. Rushforth, K. W. Edmonds, B. L. Gallagher, T. Jungwirth, Electrical switching of an antiferromagnet, Science **351**, 587 (2016).
[4] J. Železný, H. Gao, K. Výborný, J. Zemen, J. Mašek, A. Manchon, J. Wunderlich, J. Sinova, and T. Jungwirth, Relativistic Néel-order fields induced by electrical current in antiferromagnets, Phys. Rev. Lett. **113**, 157201 (2014).
[5] S. H. Yang, K. S. Ryu, and S. Parkin, Domain-wall velocities of up to 750ms^{-1} driven by exchange-coupling torque in synthetic antiferromagnets, Nat. Nanotech. **10**, 221 (2015).
[6] R. A. Duine, K.-J. Lee, S. S. P. Parkin, and M. D. Stiles, Synthetic antiferromagnetic spintronics, Nat. Phys. **14**, 217 (2018).
[7] T. Moriyama, W. Zhou, T. Seki, K. Takanashi, and T. Ono, Spin-orbit-torque memory operation of synthetic antiferromagnets, Phys. Rev. Lett. **121** 167202 (2018).
[8] T. Dohi, S. DuttaGupta, S. Fukami, and H. Ohno, Formation and current-induced motion of synthetic antiferromagnetic skyrmion bubbles, Nat. Comm. **10** 5153 (2019).
[9] C. A. Akosa, O. A. Tretiakov, G. Tatara, A. Manchon, Theory of the topological spin Hall effect in antiferromagnetic skyrmions: Impact on current-induced motion, Phys. Rev. Lett. **121** 097204 (2018).
[10] X. Zhang, Y. Zhou, and M. Ezawa, Antiferromagnetic skyrmion: stability, creation and manipulation, Sci. Rep. **6**, 24795 (2016).
[11] A. Salimath, Fengjun Zhuo, R. Tomasello, G. Finocchio, and A. Manchon, Controlling the deformation of antiferromagnetic skyrmions in the high-velocity regime, Phys. Rev. B **101**, 024429 (2020).
[12] L. Shen, J. Xia, X. Zhang, M. Ezawa, O. A. Tretiakov, X. Liu, G. Zhao, and Y. Zhou, Current-induced dynamics and chaos of antiferromagnetic bimerons, Phys. Rev. Lett. **124**, 037202 (2020).
[13] A. Mougin, M. Cormier, J. P. Adam, P. J. Metaxas, and J. Ferré, Domain wall mobility, stability and Walker breakdown in magnetic nanowires, Europhys. Lett. **78**, 57007 (2007).
[14] J. Yang, C. Nistor, G. S. D. Beach, and J. L. Erskine, Magnetic domain-wall velocity oscillations in permalloy nanowires, Phys. Rev. B **77**, 014413 (2008).
[15] O. Gomonay, T. Jungwirth, and J. Sinova, High antiferromagnetic domain wall velocity induced by Néel spin-orbit torques, Phys. Rev. Lett. **117**, 017202 (2016).
[16] S. Selzer, U. Atxitia, U. Ritzmann, D. Hinzke, and U. Nowak, Inertia-free thermally driven domain-wall motion in antiferromagnets, Phys. Rev. Lett. **117**, 107201 (2016).
[17] T. Shiino, S.-H. Oh, P. M. Haney, S.-W. Lee, G. Go, B.-G. Park, and K.-J. Lee, Antiferromagnetic domain wall motion driven by spin-orbit torques, Phys. Rev. Lett. **117**, 087203 (2016).
[18] V. Baltz, A. Manchon, M. Tsoi, T. Moriyama, T. Ono, and Y. Tserkovnyak, Antiferromagnetic spintronics, Rev. Mod. Phys. **90**, 015005 (2018).
[19] O. Gomonay, T. Jungwirth, and J. Sinova, Concepts of antiferromagnetic spintronics, physica status solidi (RRL), Rapid Research Letters **11**, 1700022 (2017).
[20] R. M. Otxoa, P. E. Roy, R. Rama-Eiroa, J. Godinho, K. Y. Guslienko, and J. Wunderlich, Walker-like domain wall breakdown in layered antiferromagnets driven by staggered spinorbit fields, Commun. Phys. **3**, 190 (2020).
[21] P. E. Roy, R. M. Otxoa, and J. Wunderlich, Robust picosecond writing of a layered antiferromagnet by staggered spin-orbit fields, Phys. Rev. B **94**, 014439 (2016).
[22] L. D. Landau and E. M. Lifshitz, On the theory of the dispersion of magnetic permeability in ferromagnetic bodies, Phys. Z. Sowjetunion **8** 153 (1935).

[23] T. L. Gilbert, A Lagrangian formulation of the gyromagnetic equation of the magnetization field, Phys. Rev. **100** 1243 (1955).

[24] S. Zhang and Z. Li, Roles of Nonequilibrium Conduction Electrons on the Magnetization Dynamics of Ferromagnets, Phys. Rev. Lett. **93** 127204 (2004).

[25] G. Tatara and H. Kohno, Theory of current-driven domain wall motion: Spin transfer versus momentum transfer, Phys. Rev. Lett. **92** 086601 (2004).

[26] See Supplemental Material at [URL inserted by publisher] for details of analytical and numerical calculations, and micromagnetic simulations. The Supplemental Material also contains Refs. [3, 5, 13, 14, 20, 29, 32].

[27] A. Thiaville, Y. Nakatani, J. Miltat, and Y. Suzuki, Micromagnetic understanding of current-driven domain wall motion in patterned nanowires, Europhys. Lett. **69**, 990 (2005).

[28] G. Tatara, C. A. Akosa, and R. M. Otxoa de Zuazola, Magnon pair emission from a relativistic domain wall in antiferromagnets, Phys. Rev. Research **2**, 043226 (2020).

[29] A. A. Thiele, Steady-state motion of magnetic domains, Phys. Rev. Lett. **30**, 230 (1973).

[30] S. Dasgupta, S. K. Kim, and O. Tchernyshyov, Gauge fields and related forces in antiferromagnetic soliton physics, Phys. Rev. B **95**, 220407 (2017).

[31] K. D. Belashchenko, O. Tchernyshyov, A. A. Kovalev, and O. A. Tretiakov, Magnetoelectric domain wall dynamics and its implications for magnetoelectric memory, Appl. Phys. Lett. **108**, 132403 (2016).

[32] H. Saarikoski, H. Kohno, C. H. Marrows, G. Tatara, Current-driven dynamics of coupled domain walls in a synthetic antiferromagnet, Phys. Rev. B **90**, 094411 (2014).

[33] G. Tatara, H. Kohno, J. Shibata, Microscopic approach to current-driven domain wall dynamics, Phys. Rep. **468**, 213 (2008).

[34] G. Tatara and R. M. Otxoa de Zuazola, Collective coordinate study of spin-wave emission from a dynamic domain wall, Phys. Rev. B **101**, 224425 (2020).

[35] K. Y. Guslienko, K. S. Lee, and S. K. Kim, Dynamic origin of vortex core switching in soft magnetic nanodots, Phys. Rev. Lett. **100**, 027203 (2008).